Faculty Publications from the Department of Electrical and Computer Engineering

Electrical & Computer Engineering, Department of

9-1-2012

Fiber-Optic Pressure Sensor Based on π-Phase-Shifted Fiber Bragg Grating on Side-Hole Fiber

Qi Zhang
University of Nebraska-Lincoln, qzhang@huskers.unl.edu

Nan Liu
University of Nebraska-Lincoln, liunan22@gmail.com

Thomas Fink
University of Nebraska-Lincoln, tfink6@gmail.com

Hong Li
Dalian University of Technology, lihongwoshi@126.com

Wei Peng
Dalian University of Technology, wpeng@dlut.edu.cn

See next page for additional authors

Follow this and additional works at: https://digitalcommons.unl.edu/electricalengineeringfacpub

Part of the Electrical and Computer Engineering Commons

Authors

Qi Zhang, Nan Liu, Thomas Fink, Hong Li, Wei Peng, and Ming Han

Fiber-Optic Pressure Sensor Based on π-Phase-Shifted Fiber Bragg Grating on Side-Hole Fiber

Qi Zhang, Nan Liu, Thomas Fink, Hong Li, Wei Peng, and Ming Han, *Member, IEEE*

Abstract—We present a fiber-optic pressure sensor based on a π-phase-shifted fiber Bragg grating (πFBG) fabricated on a side-hole fiber. Due to the resonance effect of a πFBG, its reflection spectrum features two notches that are dramatically narrower than the linewidth of a regular FBG of similar length. The narrow spectral notches allow high-resolution measurement of their spectral separation, significantly improving the pressure detection limit (defined herein as the minimum detectable pressure change) compared to sensors based on a regular FBG of a similar length and on the same fiber. The πFBG demonstrated in this letter is 8.3 mm long and the linewidth of each spectral notch is only 3.6 pm, corresponding to a quality factor of 4.3 × 10⁵. The spectral notch separation exhibited a sensitivity of 20 pm/kpsi to pressure, which was limited by the geometry of the fiber holes, and little sensitivity to temperature. The Bragg wavelength shift exhibited a sensitivity of 11.4 pm/°C to temperature. In practice, a spectral resolution of 0.028 pm can be easily achieved for the πFBG demonstrated in this letter, leading to a pressure detection limit of 1.4 psi and a temperature detection limit of 0.0025 °C.

Index Terms—Fiber Bragg grating (FBG), microstructure fiber, optical fiber sensor, π-phase-shifted fiber Bragg grating (πFBG), pressure measurement.

I. INTRODUCTION

FIBER-OPTIC pressure sensors possess many advantages over their electronic counterparts including small size, light weight, immunity to electromagnetic interference, and potential for multiplexed measurement. Owning to their great multiplexing capability, pressure sensors based on fiber Bragg gratings (FBGs) on side-hole fibers are particularly attractive for applications where a large number of sensors are desired such as industrial process control and structural health monitoring in oil wells and power plants [1]–[4].

Q. Zhang, T. Fink, and M. Han are with the Department of Electrical Engineering, University of Nebraska-Lincoln, Lincoln, NE 68588 USA (e-mail: qzhang@huskers.unl.edu; tfink6@gmail.com; mhan3@unl.edu).

N. Liu is with the Department of Mechanical and Materials Engineering, University of Nebraska-Lincoln, Lincoln, NE 68588 USA (e-mail: liunan22@gmail.com).

H. Li and W. Peng are with the College of Physics and Optoelectronic Engineering, Dalian University of Technology, Dalian 116024, China (e-mail: lihongwoshi@126.com; wpeng@dlut.edu.cn).

A side-hole fiber consists of two air channels that run through the fiber cladding and break the geometric symmetry of the fiber [5]. In the presence of hydrostatic pressure acting on the fiber surface, an anisotropic stress distribution is induced in the core, which further generates fiber birefringence via the photoelastic effect. The fiber birefringence, and consequently the hydrostatic pressure, can be measured by the separation of the FBG peaks in its reflection spectrum associated with the two polarization states. Such sensors do not require external transducers so they have the same size as the fiber and retain the mechanical, thermal, and chemical properties of the fiber. In addition, the temperature can be simultaneously measured by monitoring the Bragg wavelength shift of the FBG peak.

The pressure measurement resolution or detection limit (defined herein as the minimum detectable pressure change) of the sensor is determined by two factors: 1) the pressure sensitivity (defined herein as the spectral separation caused by unit pressure) of the side-hole fiber and 2) the resolution in measuring the relative wavelength shift of the FBG peaks. Both factors can be used to improve the overall pressure detection limit of the sensor. To improve the fiber sensitivity, several fiber designs, such as side-hole fibers with holes closer to the fiber core and of larger diameters and fibers with complicated holey structures [6], [7], have been studied. To improve the spectral measurement resolution, the FBG peak needs to be narrowed because, in many cases, the measurement resolution of the wavelength shift is highly dependent on the linewidth of the spectrum features and narrower linewidth typically leads to higher spectral resolution. For example, Hu *et. al.* [8] has shown that, given intensity noise and wavelength noise of the measurement instrumentation, the minimum detectable wavelength shift ($\Delta\lambda_{min}$) of an optical resonator sensor is inversely proportional to Q for wavelength interrogation (i.e. using a tunable laser and a photodetector) and inversely proportional to $Q^{1/2}$ for angular interrogation (i.e. using a dispersive element and an array of photodetectors), where Q is the quality factor of the resonator. Unfortunately, the spectral linewidth of FBGs with reasonable length is relatively wide (typically > 100 pm) so that the spectral measurement resolution is limited. In addition, the large linewidth makes it difficult to measure small pressure levels for which the two spectral peaks corresponding to the two polarization states cannot be easily separated.

In this letter, we propose and demonstrate a hydrostatic pressure sensor based on a short, strong π-phase-shifted

FBG (πFBG) [9] fabricated on a side-hole fiber that can significantly improve the pressure detection limit over those based on regular FBGs. The improved detection limit is due to the extremely narrow spectral notches of the πFBG reflection spectrum, which allows high-resolution measurement of the spectral separation and consequently the fiber birefringences [10]. A πFBG can be conceptually considered as a Fabry–Perot (FP) resonator formed by two FBG mirrors. When the two FBGs are highly reflective, the Q of the FP cavity is increased, leading to spectral notches dramatically narrower than the spectral linewidth of a regular FBG of similar length. The short πFBG demonstrated in this letter, is 8.3 mm long but features a narrow linewidth of only 3.6 pm for each of the two spectral notches at center wavelength of $\sim$1544 nm. The linewidth corresponds to a cavity Q of 4.3×10^5 and is tens of times narrower than the linewidth of a regular FBG of similar length. We studied the spectral notch separation for differential pressure from 0 to 1000 psi and temperature from room temperature to 200 °C. Due to the high spectral resolution, a side-hole fiber with relatively small hole diameters can be used and the spectral notch separation has little cross-sensitivity to temperature variations. Additionally, we demonstrate that the temperature can be measured with high resolution as well by monitoring the shift of the Bragg wavelength. Similar to FBG-based pressure sensors, the proposed πFBG pressure sensor has excellent multiplexing capability.

II. Sensor Fabrication

A πFBG was fabricated on a side-hole fiber using a setup schematically shown in Fig. 1, which consists of a scanning UV beam at wavelength of 193 nm, a movable aperture, and a phasemask on a high-precision linear translational stage. The linear stage allows precise movement of the phasemask on the nanometer level. The fiber was placed in front of the phasemask. To fabricate the grating, first the UV laser was focused onto the fiber through a cylindrical lens (not shown in Fig. 1) and scanned over the aperture to inscribe half of the grating. Then the phasemask was moved by a distance of $\Lambda/2$ along the fiber axis to introduce the π phase shift, where $\Lambda = 533.5$ nm in our experiment is the pitch size of the grating. After the movement of the phasemask, the aperture was positioned to inscribe the other half of the grating, and the UV laser was scanned again. The use of the 193 nm laser allows us to fabricate strong gratings on standard Germanium-doped fibers without photosensitization [11], [12].

Using the setup, we fabricated an 8.3-mm long πFBG with narrow spectral notches on a side-hole fiber for high-resolution hydrostatic pressure measurement. Figure 2a is a picture of the side-hole fiber used in the experiment. The fiber diameter is 125 μm, same as that of a conventional single mode fiber. Both holes have diameters of $\sim$26 μm and the distance between the center of the hole and the fiber axis is $\sim$26 μm. Figure 2b and c show, respectively, the transmission spectrum measured by an optical spectrum analyzer (OSA) and the reflection spectrum measured by a sensor interrogator of the πFBG. The depth of the transmission spectrum is >35 dB, indicating a max-
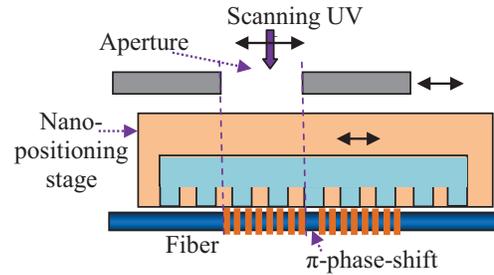

Fig. 1. Schematic of πFBG fabrication using a scanning UV laser and a phasemask on a nanopositioning stage.
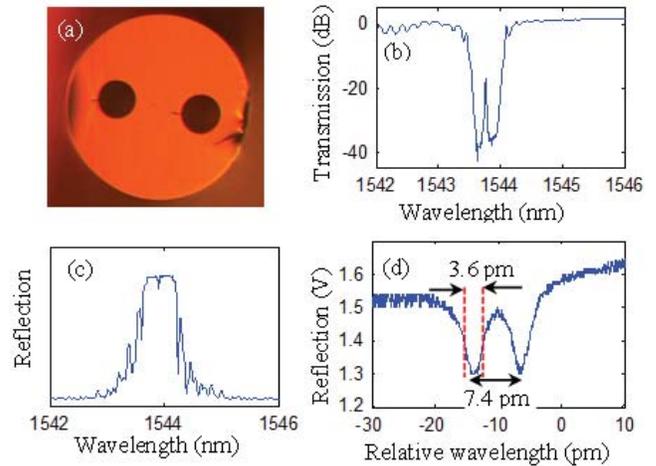

Fig. 2. (a) Picture of the side-hole fiber. (b) Transmission spectrum. (c) and (d) Reflection spectrum of a πFBG fabricated on the side-hole fiber.

imum reflectivity of >99.96% for the πFBG. The transmission peak at the center of the spectrum of the πFBG is evident. It is worth noting that due to the limited resolution of the OSA (20 pm) and the sensor interrogator (5 pm), only a single transmission peak was observed in Fig. 2b and c. The spectral details around the center of the reflection spectrum were studied using a narrow-linewidth (<300 kHz) wavelength-tunable diode laser and is shown in Fig. 2d, which clearly shows the two reflection notches associated with the two polarization states. We estimated the spectral separation of the two notches to be 7.4 pm and the full-width-at-half-maximum (FWHM) of each notch to be 3.6 pm, leading to a cavity Q of 4.3×10^5. We note that the two spectral notches were completely separated even when no pressure was applied. As a result, the sensor can measure small or even negative differential pressures.

To take advantage of the high-Q of a πFBG sensor, a wavelength interrogation scheme is required. [8] Such a scheme typically uses a wavelength scanning laser and a photodetector. Frequency-modulation spectroscopy in which the laser frequency scanning is achieved through an optical modulator powered by a scanning rf source can also be used [13], [14] It is worth noting that angular interrogation schemes, which use a dispersive element and an array of photondetectors, are suitable for interrogation of regular FBGs but may not have the resolution for a high-Q sensor.

III. EXPERIMENTAL RESULTS

We tested the pressure response of the sensor in a pneumatic pressure chamber at room temperature. The differential pressure was increased from 0 to 1000 psi. The pressure was monitored by a pressure gauge with an accuracy of 6 psi. The same narrow-linewidth tunable laser used to obtain Fig. 2d was used to measure the reflection spectrum of the πFBG. Before each measurement, the light polarization was tuned so that both spectral notches were observed with similar depth. Figure 3a gives the reflection spectra at pressure levels of 30, 350, 650, and 1000 psi and clearly shows that the separation of the two spectral notches increases as the differential pressure increases. To calculate the spectral separation at a given pressure, we used a second-order polynomial fit to the data around the notch wavelength for each notch. Figure 3b shows the spectral notch separation as a function of differential pressure. The least-square linear fit of the curve indicates that the sensor has a pressure sensitivity of 20 pm/kpsi and the linearity of the pressure response curve has a correlation coefficient $R = 0.9995$ over the whole measurement range.

Although the pressure sensitivity of the side-hole fiber used here is smaller compared to those in other works where side-hole fibers with larger holes were used [2], [4], the sensor demonstrated here can still achieve excellent pressure detection limit due to the significantly improved spectral resolution by the use of a strong πFBG with high Q and extremely narrow spectral notches. As an estimation, we assume the sensor is interrogated by a wavelength interrogation scheme in which a wavelength tunable laser with a spectral width of $\sim$2.6 pm and wavelength repeatability of 0.1 pm is used, it is shown that a resolution of the spectral measurement down to 0.028 pm can be achieved by a 16-scan averaging for a resonator with $Q = 4.3 \times 10^5$ (Ref. [8]), same as the Q of the πFBG sensor demonstrated in this letter. Considering the pressure sensitivity of 20 pm/kpsi of the side-hole fiber used here, a pressure detection limit of 1.4 psi can be achieved.

To evaluate the temperature cross-sensitivity of the proposed pressure sensor, we measured the separation of the spectral notches as a function of temperature at ambient pressure. The temperature was increased from 25 to 200 °C. The results are shown in Fig. 4. The scale of the vertical axis is the same as in Fig. 3b for comparison. It is seen that the separation of the spectral notches showed little sensitivity to temperature within the temperature range. The small temperature cross-sensitivity can be attributed to the relatively small diameters of the holes in the side-hole fiber.

Although the spectral separation of the two notches is insensitive to temperature, their absolute spectral positions are highly sensitive to temperature. To demonstrate the temperature sensing capability, we measured the Bragg wavelength shift as a function of temperature using the same sensor interrogator in obtaining Fig 2c. Figure 5a shows the reflection spectra at several temperatures. To find the Bragg wavelength at each temperature, a second-order polynomical fit was applied to the notch of the curve shown in Fig. 5a. Figure 5b shows the Bragg wavelength as a function of temperature with its linear fitting. The results indicate that the πFBG has a
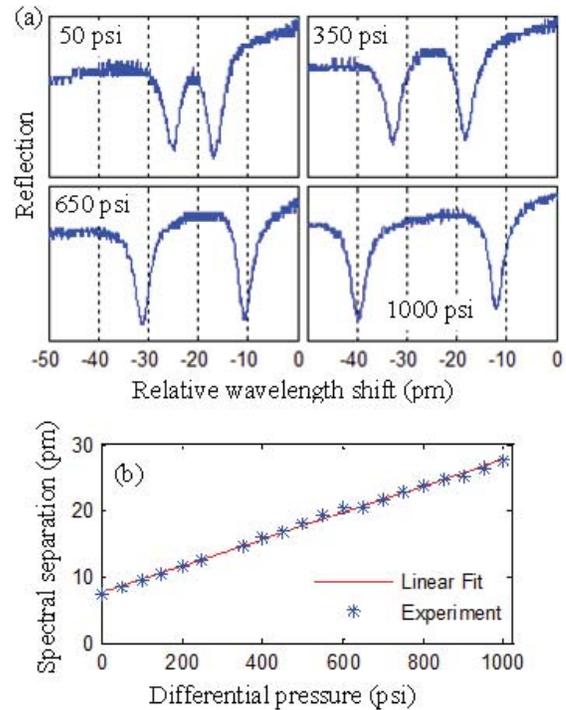

Fig. 3. (a) πFBG reflection spectra at different pressure levels. (b) Separation of πFBG spectral notches versus differential pressure.
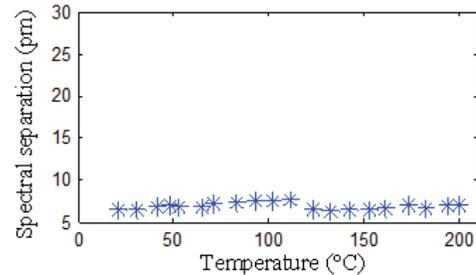

Fig. 4. Separation of the spectral notches of the πFBG versus temperature.

temperature sensitivity of 11.4 pm/°C. Due to the narrow width of the spectral notch, we expect that the πFBG potentially can have a much higher resolution for temperature measurement than regular FBGs with similar length. Assuming that we use the same wavelength interrogation scheme and the same spectral measurement resolution of 0.028 pm as in estimating the pressure detection limit, a temperature detection limit of 0.0025 °C can be achieved.

IV. NUMERICAL VERIFICATION

To numerically validate the sensor response to pressure, finite-element analysis was carried out to simulate the strain field distribution over the fiber cross-section at a given pressure, from which the spectral separation of the two πFBG notches can be calculated. The geometric parameters of the fiber, shown in Fig. 6a, are similar to those of the fiber used in the experiment. Young's modulus $E = 73$ GPa and Poisson's ratio $\nu = 0.17$ were assumed for both the cladding and the core of the fiber.
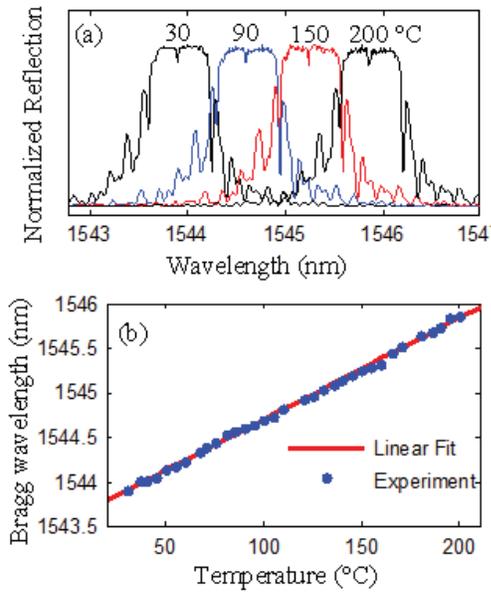
Fig. 5. (a) πFBG reflection spectra at several temperatures. (b) Experimental results and linear fit of πFBG Bragg wavelength versus temperature.
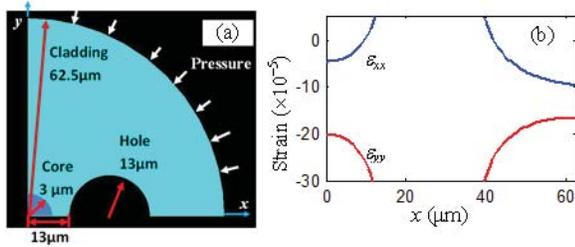

Fig. 6. (a) Fiber geometry (only a quarter of the fiber cross section is shown) used in the analysis. (b) Simulation results of the strain field distribution along the x-axis.

Figure 6b shows the normal strain field distribution along x-axis (defined by the centers of the two holes) induced by a hydrostatic pressure of $P = 10$ MPa (1450 psi). The normal strains at the fiber axis are $\varepsilon_{xx} = -4.75\times10^{-5}$ and $\varepsilon_{yy} = -20.0\times10^{-5}$. In a single-mode fiber of core index n, the elasto-optic index changes, δn_x and δn_y, can be evaluated by [15]

$$\delta n_i = -\left(n^3 \big/ 2\right) \sum\nolimits_{ij} p_{ij}\varepsilon_{ij} \qquad (1)$$

where p_{ij} are the strain-optic coefficients of the fiber material. The position of the πFBG spectral notches are given by $\lambda_i = 2n_i\Lambda$, from which the separation of the πFBG spectral notches is evaluated by

$$\Delta\lambda = \lambda_x - \lambda_y = -n^3\left(p_{11} - p_{12}\right)\left(\varepsilon_{xx} - \varepsilon_{yy}\right)\Lambda. \qquad (2)$$

Using the simulated strain values and the following parameters for fused silica and the πFBG: $p_{11} = 0.121$, $p_{12} = 0.270$, $n = 1.446$, and $\Lambda = 533.5$ nm in (2), we obtain that the 10 MPa pressure causes 34.8 pm separation of the πFBG spectral notches, corresponding to a pressure sensitivity of 25 pm/kpsi, which agrees reasonably well with the experimental result of 20 pm/kpsi.

V. Conclusion

We proposed and demonstrated a fiber-optic hydrostatic pressure sensor based on a high-Q πFBG on a side-hole fiber. The reflection spectrum of a πFBG features two narrow spectral notches, the separation of which is dependent on the fiber birefringence caused by the pressure applied on the side-hole fiber. Due to the narrow linewidth of the spectral notches, small separation can be detected, leading to high-resolution pressure measurement. The sensor demonstrated in this letter has an 8.3-mm long πFBG and a linewidth of 3.6 pm for each spectral notch, corresponding to a cavity Q of 4.3×10^5. The spectral notch separation exhibited a sensitivity of 20 pm/kpsi to pressure and little sensitivity to temperature. The Bragg wavelength shift exhibited a sensitivity of 11.4 pm/°C to temperature. For the πFBG demonstrated here, a spectral resolution of 0.028 pm can be easily achieved using a wavelength interrogation scheme, leading to a pressure detection limit of 1.4 psi and a temperature detection limit of 0.0025 °C. The measured pressure sensitivity agrees well with the theoretical results obtained by finite-element analysis.

References

[1] S. Kreger, S. Calvert, and E. Udd, "High pressure sensing using fiber Bragg gratings written in birefringent side hole fiber," in *15th Opt. Fiber Sensors Conf. Tech. Dig.*, vol. 1. 2002, pp. 355–358.

[2] T. Chen, *et al.*, "Regenerated gratings in air-hole microstructured fibers for high-temperature pressure sensing," *Opt. Lett.*, vol. 36, no. 18, pp. 3542–3544, 2011.

[3] C. M. Jewart, *et al.*, "Ultrafast femtosecond-laser-induced fiber Bragg gratings in air-hole microstructured fibers for high-temperature pressure sensing," *Opt. Lett.*, vol. 35, no. 9, pp. 1443–1445, 2010.

[4] E. Chmielewska, W. Urbanczyk, and W. J. Bock, "Measurement of pressure and temperature sensitivities of a Bragg grating imprinted in a highly birefringent side-hole fiber," *Appl. Opt.*, vol. 42, no. 31, pp. 6284–6291, 2003.

[5] H. M. Xie, *et al.*, "Side-hole fiber for fiberoptic pressure sensing," *Opt. Lett.*, vol. 11, no. 5, pp. 333–335, 1986.

[6] S. Sulejmani, *et al.*, "Control over the pressure sensitivity of Bragg grating-based sensors in highly birefringent microstructured optical fibers," *IEEE Photon. Technol. Lett.*, vol. 24, no. 6, pp. 527–529, Mar. 15, 2012.

[7] J. R. Clowes, S. Syngellakis, and M. N. Zervas, "Pressure sensitivity of side-hole optical fiber sensors," *IEEE Photon. Technol. Lett.*, vol. 10, no. 6, pp. 857–859, Jun. 1998.

[8] J. J. Hu, *et al.*, "Design guidelines for optical resonator biochemical sensors," *J. Opt. Soc. Amer. B*, vol. 26, no. 5, pp. 1032–1041, 2009.

[9] J. Canning and M. G. Sceats, "Pi-phase-shifted periodic distributed structures in optical fFibers by UV post-processing," *Electron. Lett.*, vol. 30, no. 16, pp. 1344–1345, 1994.

[10] M. LeBlanc, *et al.*, "Transverse load sensing by use of pi-phase-shifted fiber Bragg gratings," *Opt. Lett.*, vol. 24, no. 16, pp. 1091–1093, 1999.

[11] B. Malo, *et al.*, "Enhanced photosensitivity in lightly doped standard telecommunication fiber exposed to high fluence ArF excimer-laser light," *Electron. Lett.*, vol. 31, no. 11, pp. 879–880, 1995.

[12] J. Albert, *et al.*, "Comparison of one-photon and 2-photon effects in the photosensitivity of germanium-doped silica optical fibers exposed to intense ArF excimer-laser pulses," *Appl. Phys. Lett.*, vol. 67, no. 24, pp. 3529–3531, 1995.

[13] G. C. Bjorklund, "Frequency-modulation spectroscopy − new method for measuring weak absorptions and dispersions," *Opt. Lett.*, vol. 5, no. 1, pp. 15–17, 1980.

[14] D. Y. Stepanov, J. Canning, and Z. Brodzeli, "Real-time characterisation of fibre grating Fabry–Perots and phase-shifted gratings with 100 kHz resolution," in *NIST Tech. Dig. Symp. Opt. Fiber Meas.*, 1998, pp. 149–152.

[15] J. F. Nye, *Physical Properties of Crystals*. London, U.K.: Clarendon, 1969.